Hindawi Publishing Corporation
Advances in Meteorology
Volume 2016, Article ID 3282064, 13 pages
http://dx.doi.org/10.1155/2016/3282064

Research Article

Evaluation of the Impacts of Assimilating the TAMDAR Data on 12/4 km Grid WRF-Based RTFDDA Simulations over the CONUS

Yongxin Zhang,[1] Yubao Liu,[1] and Thomas Nipen[2]

[1]*Research Applications Laboratory, National Center for Atmospheric Research, Boulder, CO, USA*
[2]*Norwegian Meteorological Institute, Henrik Mohns Plass 1, 0313 Oslo, Norway*

Correspondence should be addressed to Yongxin Zhang; zhangyx@ucar.edu

Received 25 April 2016; Accepted 8 August 2016

Academic Editor: Rossella Ferretti

An analysis of the impacts of assimilating the Tropospheric Airborne Meteorological Data Report (TAMDAR) data with the Weather Research and Forecasting- (WRF-) real-time four-dimensional data assimilation (RTFDDA) and forecasting system over the Contiguous US (CONUS) is presented. The impacts of the horizontal resolution increase from 12 km to 4 km on the WRF-RTFDDA simulations are also examined in conjunction with the TAMDAR data impacts. The assimilation of the TAMDAR data reduces the root mean squared error of the moisture field predictions and increases the correlation between the predictions and the observations for both domains with 12 km and 4 km grid spacings. The TAMDAR data reduce the model dry biases in the middle and lower levels by adding moisture at those levels. Assimilating the TAMDAR data improves temperature predictions at middle to high levels and wind speed predictions at all levels especially for the 12 km domain. Increasing the horizontal resolution from 12 km to 4 km results in significantly larger impacts on surface variables than assimilating the TAMDAR data.

1. Introduction

The steady accumulation of evidence has long suggested that the accurate specification of the initial atmospheric conditions in numerical weather prediction (NWP) models through data assimilation of observations can greatly improve short-term weather forecasts (e.g., [1–3]). However, upper-air observations are disproportionately sparse, both temporally and geographically, when compared to surface observations. Traditionally, upper-air observations are obtained primarily through the rawinsonde networks at two standard launch times, 0000 Coordinated Universal Time (UTC) and 1200 UTC. The rawinsonde networks tend to have large variations in spatial distributions depending on the country and the region that operate them. The inclusion of automated weather reports from commercial aircraft worldwide as part of the Aircraft Meteorological Data Relay (AMDAR) program started more than a decade ago and it has been an important data source for numerical weather prediction [4]. Many studies have found positive impacts from using automated aircraft data in NWP systems (e.g., [5–12]). However, most aircraft data are gathered at cruising levels (7500–13500 m above sea level), and below about 7500 m, aircraft data are mainly concentrated near major airport hubs over the Contiguous United States (CONUS) and other limited regions [4]. Another weakness of the current AMDAR dataset is the almost complete absence of water-vapor data at any altitude [4].

Recently, as a joint effort among the National Aeronautics and Space Administration (NASA), the Federal Aviation Administration (FAA), the National Oceanic and Atmospheric Administration (NOAA), and AirDat LLC (http://www.airdat.com/), the Tropospheric Airborne Meteorological Data Reporting (TAMDAR) project was established [13–15]. The TAMDAR sensors are specifically designed to instrument smaller commercial aircraft that fly in the lower and middle troposphere with frequent ascents and descents over the CONUS and other parts of the world [16]. TAMDAR provides measurements of humidity, pressure, temperature, and winds as well as icing and turbulence during the ascents, descents, and cruises of aircraft. The TAMDAR sensors were initially deployed on a fleet of 63 Saab 340s operated by Mesaba Airlines in the Great Lakes region but have since been expanded to be included in many other airlines over North

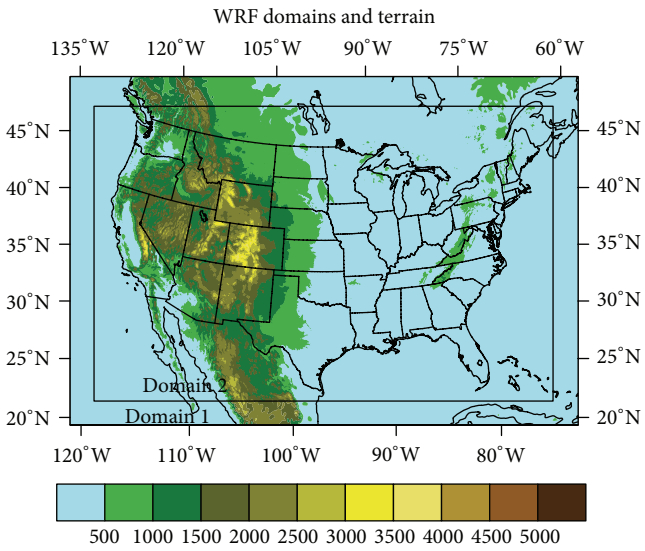

Figure 1: WRF-RTFDDA model domains with one nest (Domain 1: 12 km; Domain 2: 4 km). Shades represent terrain height (m) for the corresponding WRF domain.

America, Hawaii, Caribbean, and Europe. Aircraft equipped with the TAMDAR sensors typically fly regional routes at altitudes generally below 7500 m, thus effectively filling in the spatial data voids of the AMDAR flights and the temporal data voids of the rawinsonde networks. Preliminary studies using the TAMDAR data in a real-time four-dimensional data assimilation (RTFDDA) and forecasting system showed positive impacts of the TAMDAR data on mesoscale analyses and simulations [14, 17–20]. Subsequent analyses of the TAMDAR data impacts using different data assimilation systems have also shown encouraging results on NWP forecasts over the CONUS [21, 22] and on hurricane track predictions [23].

Building on the works of Liu et al. [17, 18] and Jacobs et al. [14], the National Center for Atmospheric Research (NCAR) and AirDat LLC started in July 2009 a collaboration that led to the development of the operational NWP forecasts for the CONUS domain at 12 km and 4 km resolution (Figure 1) using the Weather Research and Forecasting- (WRF-) based RTFDDA analysis and forecasting system [24, 25]. This system, herein referred to as NCAR-AirDat RTFDDA, assimilates available observations from a variety of observation networks as well as the TAMDAR winds, temperature, and humidity. The choice of the 4 km resolution for the inner CONUS domain is based on the findings of Weisman et al. [26] who suggest that 4 km is sufficient to reproduce the mesoconvective circulations and net momentum and heat transport of midlatitude type convective systems. In this NCAR-AirDat RTFDDA system, the 12 km domain uses both the Kain-Fritsch cumulus parameterization [27–29] and the Lin et al. microphysics scheme [30–32] while the 4 km domain only uses the Lin et al. microphysics scheme. Hong and Pan [33] suggest that, in a mesoscale model with horizontal resolution on the order of tens of kilometers, a proper treatment of subgrid-scale precipitation physics is crucial to provide the favorable synoptic conditions for grid-resolvable precipitation physics to be activated at the correct location. The high-resolution TAMDAR data both spatially and temporally are expected to have larger impacts with explicit cloud physics than with cumulus parameterization. In this work, we analyze the impacts of both the TAMDAR data and the resolution increase from 12 km to 4 km on the RTFDDA simulations.

The focus of this work is twofold: (1) documenting the design of the NCAR-AirDat RTFDDA system and (2) examining the impact of the TAMDAR data and the model resolution increase on the RTFDDA simulations based on 6-day parallel simulations with and without using the TAMDAR data. The 6-day study period is arbitrarily chosen. What distinguishes this work from the aforementioned papers on the TAMDAR data impact is that in this work the TAMDAR data impacts are evaluated in a real-time operational system and that the impacts are evaluated in terms of percentage improvement (or percentage degradation). Furthermore, the TAMDAR data impact is examined in the context of the model resolution increase from 12 km to 4 km with differing cloud physics. The paper is organized as follows. Section 2 briefly describes the RTFDDA system. The experimental design is discussed in Section 3. Section 4 examines the impact of the TAMDAR data and the resolution increase on the RTFDDA simulations. Conclusions and discussions are included in Section 5.

2. The RTFDDA System

RTFDDA is a version of the four-dimensional weather system that was developed by NCAR in collaboration with the US Army Test and Evaluation Command. The RTFDDA system was originally built upon the fifth-generation Pennsylvania State University-NCAR Mesoscale Model (MM5, [34]) and was described in detail by Cram et al. [35] and later by Liu et al. [36]. The core of the RTFDDA system is a data assimilation component that continuously assimilates meteorological observations as they become available, thereby producing model-observation integrated 4D datasets that both define the current atmospheric conditions and serve as the initial conditions for subsequent model forecasts. This approach effectively alleviates the spin-up issue in short-term weather forecasting as continuous assimilation provides initial conditions that are consistent with both the dynamic equations in the model and the atmospheric states provided by the observations.

The data assimilation component in RTFDDA employs the Newtonian relaxation approach that uses nonphysical nudging terms in the model predictive equations [36]. These nudging terms synchronize the model atmospheric states at each grid point towards the observations in proportion to the differences between the model solutions and the observations [37]. Each observation affects the model states in proportion to the temporal and spatial weights that are maximized at its observed time and location, and the model spreads the observed information in time and space according to the model dynamics. The data utilized by the assimilation system include the standard hourly surface reports and twice-daily

rawinsondes; data from mesoscale networks; wind profiler data; hourly cloud-track winds derived from infrared, visible, and water-vapor satellite images; and aircraft reports. The ability of RTFDDA to ingest and weight each observation uniquely according to its observation time and location permits the effective and accurate assimilation of the observations from continuously moving platforms such as TAMDAR.

Applications of the RTFDDA system include Davis et al. [38] on mesoscale predictability over complex terrain and heterogeneous land surfaces, Warner and Hsu [39] on simulations of moist convection over the Southwestern US, Rife et al. [40] on diurnal boundary layer circulations in the Great Basin Desert, Rife et al. [41] on the predictability of low-level winds over the Salt Lake valley and surrounding mountains, and Warner et al. [42] on emergency-response applications of high-resolution mesoscale simulations through graphical interfaces. Liu et al. [17, 18] update the RTFDDA system by improving the nonlocal planetary boundary layer (PBL) parameterization scheme and the National Centers for Environmental Prediction- (NCEP-) Oregon State University-Air Force-Hydrologic Research Laboratory (NOAH) land surface model (LSM). The improvements involve implementation of a better representation of surface-layer momentum fluxes, a more accurate diagnosis of the boundary layer depth, and a bulk parameterization of urban substrate properties in the LSM. Validations of the RTFDDA simulations for the Oklahoma City area during the Joint Urban 2003 Field Project show quite satisfactory performance of the model system in resolving the observed surface variables and mesoscale circulations associated with an urban environment [17, 18].

The RTFDDA system was subsequently set up for operational runs at five US Army test ranges starting in 2001 and the characteristics and performance of the system during the multiyear operational runs have been documented in a series of papers. Liu et al. [36], the first of the series, report the design of the modeling system for each test range and the effective use of the forecast products for satisfying a variety of needs. In the second paper [43], evaluations of the RTFDDA system at the five test ranges using wind, temperature, and specific humidity observations are presented. The last of the series, Sharman et al. [44], documents the use of the model forecasts to drive secondary-application models such as a sound propagation model, a missile trajectory model, and a transport and diffusion model for daily decision-making. These papers confirm the previous findings that the RTFDDA system is able to resolve the fine circulations associated with local complex terrain, though varying degrees of differences in forecast errors from range to range, within the diurnal cycles, with elapsed forecast time, and among the seasons are noted. Furthermore, these papers show that the accuracies of the secondary-application forecasts driven by the RTFDDA simulations are sufficient to meet operational needs in most cases.

Succeeding MM5 as the community weather model, the multiagency sponsored WRF model has been integrated into the RTFDDA framework as the data assimilation and forecast driving engine. The implementation, evaluation, and refinement of the WRF-based RTFDDA system at US Army test ranges and other locations are presented in Liu et al. [19, 20] and Liu et al. [45]. WRF is a mesoscale NWP system designed for both short-term weather forecasts and long-term climate simulations with horizontal resolutions ranging from meters to thousands of kilometers (http://www.wrf-model.org/). It is a nonhydrostatic model and has a two-way interactive nesting procedure with coarse grids providing boundary conditions for fine grids and with feedback from fine grids to coarse grids. Model physics include microphysics, cumulus parameterization, PBL, LSM, and longwave and shortwave radiation [46].

3. Experimental Design

WRF-RTFDDA was set up for the AirDat real-time operational runs over the CONUS domain with the purpose of (a) assimilating the TAMDAR data and (b) providing high-resolution daily numerical weather forecasts for the CONUS [25]. The system uses nested domains with a coarse grid at 12 km and a fine grid at 4 km horizontal resolution (Figure 1). In contrast to the typical offline one-way nested-grid simulation method by which the nested-grid domains are run subsequently, the WRF online one-way nested-grid strategy by which all nested-grid domains run simultaneously and the coarse-grid domain provides the boundary conditions for the fine-grid domains at every time step is employed. The one-way nesting was chosen in order to obtain both the explicit (on the 4 km fine-grid domain) and implicit (on the 12 km coarse-grid domain) cloud/precipitation forecasts for the CONUS area and provide an opportunity to assess the benefit of the high-resolution model runs with explicit cloud physics and, in particular, the TAMDAR data impact on the simulation of convective systems. Both domains cover the entire Contiguous US (CONUS) and Northern Mexico and Southern Canada. Both domains do not extend considerably to the data-void oceanic areas, that is, the East Pacific Ocean, the West Atlantic Ocean, and the Gulf of Mexico.

The operational runs of the NCAR-AirDat WRF-based RTFDDA system were started in July 2009 and have been running continuously since then. The model forecasts are cycled at a time interval of 6 hours, started at 00Z, 06Z, 12Z, and 18Z, respectively, and, in each cycle, 6 h final analyses for the past 6 h (−6 h to 0 h) and 24 h forecasts (72 h forecasts since March 2010) are generated. For examining the impact of the TAMDAR data on the real-time RTFDDA simulations, two parallel runs in an operational mode with and without assimilating the TAMDAR data while keeping everything else the same were conducted for August 1 through August 6, 2009 (6 days). The study period was chosen randomly for the summer convective weather conditions. Due to the consideration of computing time and disk space, the parallel runs were conducted for 6 days only. Admittedly, a 6-day period is too short for a systematic evaluation of the TAMDAR data impact in an operational setting; however, we would argue that the randomly chosen time period appears adequate for looking at the essential picture of the TAMDAR data impact for the summer convective season.

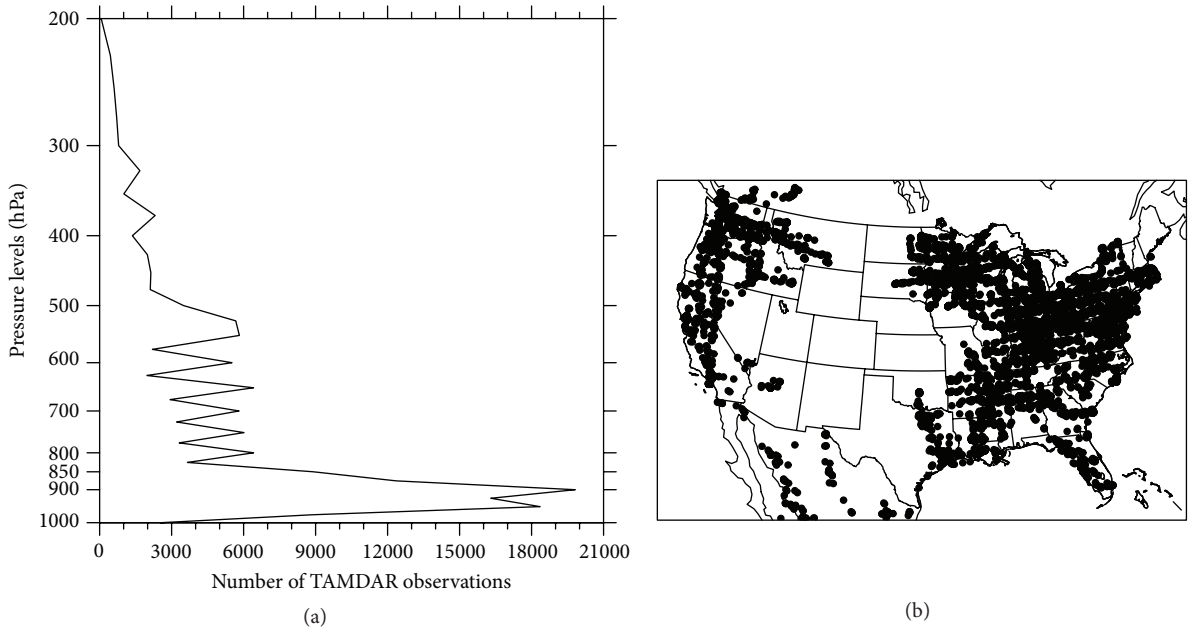

Figure 2: Vertical distributions of the number of the TAMDAR observations (a) and horizontal coverage of the TAMDAR observations (b) during August 1 through 6, 2009 (plotted every 12th point).

Figure 2 shows the vertical and horizontal distributions of the TAMDAR reports over the CONUS during the period of August 1 through August 6, 2009. A majority of the TAMDAR reports are located below 850 hPa, although a small number of reports can also be found up to 200 hPa (Figure 2(a)). Horizontally, most of the TAMDAR reports are obtained over the Eastern US, the states of California, Oregon, and Washington, with the Central US being the TAMDAR data-void area during the simulation period (Figure 2(b)).

All of the 24 h forecasts of each cycle (4 cycles per day) and the standard radiosondes and surface observations from the WMO's (World Meteorological Organization's) Global Telecommunication System (GTS) were used to compute the verification statistics during the simulation period.

4. Impacts of the TAMDAR Data and Resolution Increase on the RTFDDA Simulations

The RTFDDA simulations from sensitivity experiments with and without assimilating the TAMDAR data are verified against all available radiosonde observations and surface observations over the CONUS. The verification is conducted for both the coarse grid at 12 km resolution and the fine grid at 4 km resolution using the same observation data. The impact of the resolution increase from 12 km (i.e., Domain 1) to 4 km (i.e., Domain 2) on the RTFDDA simulations is also examined. By investigating the impacts of the TAMDAR data in conjunction with those of the resolution increase, the relative importance of the TAMDAR data versus horizontal resolution in improving model forecasts could be revealed. For the verification study, the model outputs are interpolated to observation station locations using the bilinear method. Skill scores (SS, i.e., percentage improvement) of root mean squared error (RMSE) and forecast-observation correlation are computed to quantify the impacts of the TAMDAR data and the resolution increase. The percentage improvements are averaged over all station locations, the 24 forecast hours, and the 6-day simulation period. The skill score in RMSE resulting from assimilating the TAMDAR data ($\mathrm{SSRMSE_{TAMDAR}}$) and from the resolution increase ($\mathrm{SSRMSE_{RESOLUTION}}$) is defined as follows:

$$\begin{aligned}&\mathrm{SSRMSE_{TAMDAR}}\\&\quad = 100\% \times \frac{\left(\mathrm{RMSE_{noTAMDAR}} - \mathrm{RMSE_{TAMDAR}}\right)}{\mathrm{RMSE_{noTAMDAR}}},\\&\mathrm{SSRMSE_{RESOLUTION}}\\&\quad = 100\% \times \frac{\left(\mathrm{RMSE_{Domain1}} - \mathrm{RMSE_{Domain2}}\right)}{\mathrm{RMSE_{Domain1}}}.\end{aligned} \tag{1}$$

Thus, positive (negative) values represent positive (negative) impacts of assimilating the TAMDAR data or resolution increase on reducing the model RMSE.

The forecast-observation correlation improvement is defined as

$$\begin{aligned}\mathrm{CCI_{TAMDAR}} &= \mathrm{Correlation_{TAMDAR}}\\&\quad - \mathrm{Correlation_{noTAMDAR}},\\\mathrm{CCI_{RESOLUTION}} &= \mathrm{Correlation_{Domain2}}\\&\quad - \mathrm{Correlation_{Domain1}},\end{aligned} \tag{2}$$

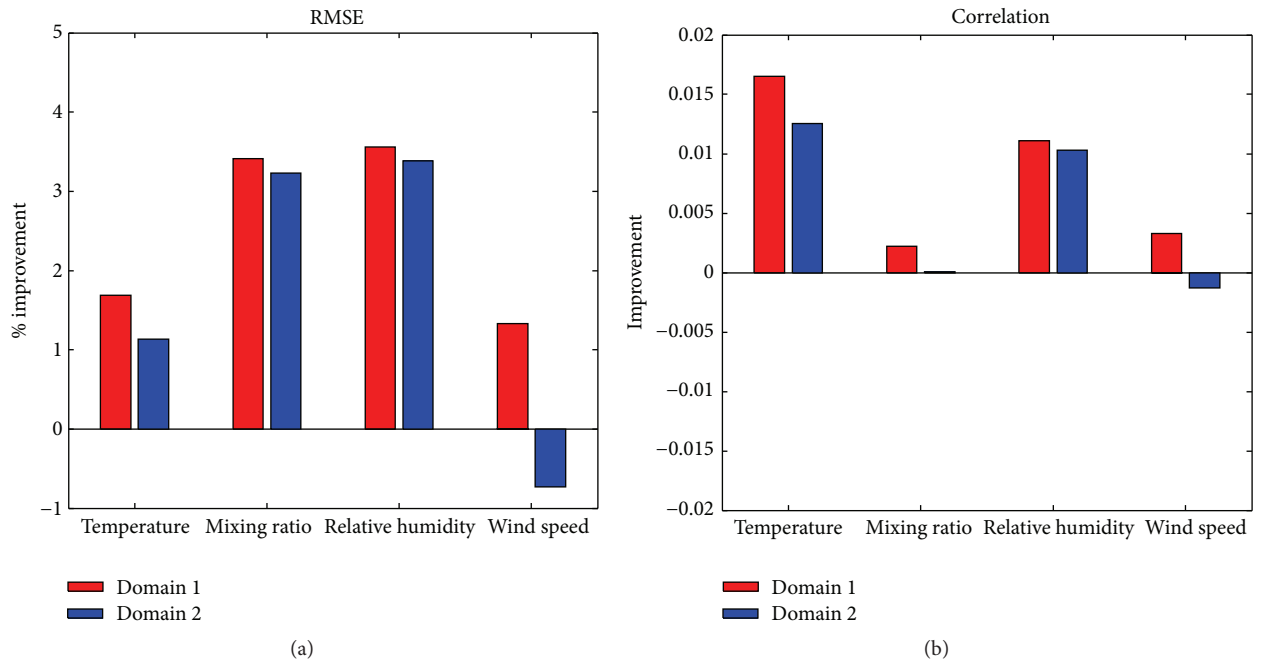

Figure 3: (a) Percentage improvements for root mean squared error (RMSE) and (b) correlation improvement for temperature, mixing ratio, relative humidity, and wind speed due to the assimilation of the TAMDAR data (Domain 1: red bars; Domain 2: blue bars). The abscissa represents the variables while the ordinate represents the improvement. The statistics are averaged over all sounding locations, the 400–600 hPa layer, and the 6-day (August 1 through August 6) simulation period.

where Pearson's correlation coefficient for each station location is defined as

$$\mathrm{CC} = \frac{\sum_{i=1}^{n} \left(x_o^i - \overline{x}_o\right)\left(x_m^i - \overline{x}_m\right)}{\sqrt{\sum_{i=1}^{n} \left(x_o^i - \overline{x}_o\right)^2 \sum_{i=1}^{n} \left(x_m^i - \overline{x}_m\right)^2}}, \quad (3)$$

with i referring to the number of samples at the station, subscripts o denoting the observations, and m denoting the model forecasts.

Likewise, positive (negative) values of the correlation improvement represent positive (negative) impacts of assimilating the TAMDAR data or resolution increase on increasing the correlation between the simulations and the observations. Examined variables include temperature, mixing ratio, relative humidity, and wind speed in the case of vertical profiles, with the addition of surface pressure in the case of surface variables.

4.1. Overall Impacts. Figure 3 shows the percentage improvements for RMSE and correlation improvement for temperature, mixing ratio, relative humidity, and wind speed averaged over the 400–600 hPa layer due to the assimilation of the TAMDAR data. This layer corresponds to where the impacts of the TAMDAR data on the model simulations appear to be noticeable for most of the examined variables as will be discussed later. For temperature (Figure 3(a)), positive impacts on RMSE are noted for both Domain 1 and Domain 2, with Domain 1 showing relatively bigger impacts than Domain 2. Correlation analysis also indicates large positive impacts on temperature for both domains (Figure 3(b)).

For mixing ratio, assimilating the TAMDAR data has significantly positive impacts on reducing the RMSE for both domains (Figure 3(a)), with slightly positive impacts in terms of correlation improvement for Domain 1 (Figure 3(b)). For relative humidity, large positive impacts are noted for both RMSE and correlation (Figures 3(a) and 3(b)). The reason that correlation improvement shows larger positive impacts for relative humidity than mixing ratio is likely related to the fact that relative humidity is directly observed by the TAMDAR sensors while mixing ratio is derived from the observed relative humidity in the modeling system, which can be affected by the forecast errors of temperature and pressure fields. Thus, improving the model temperature and pressure analyses and forecasts will directly increase the effectiveness of assimilating the TAMDAR relative humidity measurements. Small but tangible differences in the moisture fields are also noted between Domain 1 and Domain 2 (Figures 3(a) and 3(b)). While both the cumulus parameterization and microphysics schemes are used in Domain 1 to simulate the cloud/precipitation processes, Domain 2 uses only the microphysics scheme, which permits more realistic interaction between the TAMDAR moisture and model clouds and thus results in more realistic structure and evolution of summer convection over the CONUS as will be discussed in a separate paper.

Assimilating the TAMDAR data reduces the RMSE and improves the correlation for wind speed for Domain 1 (Figures 3(a) and 3(b)). For Domain 2, slightly negative impacts

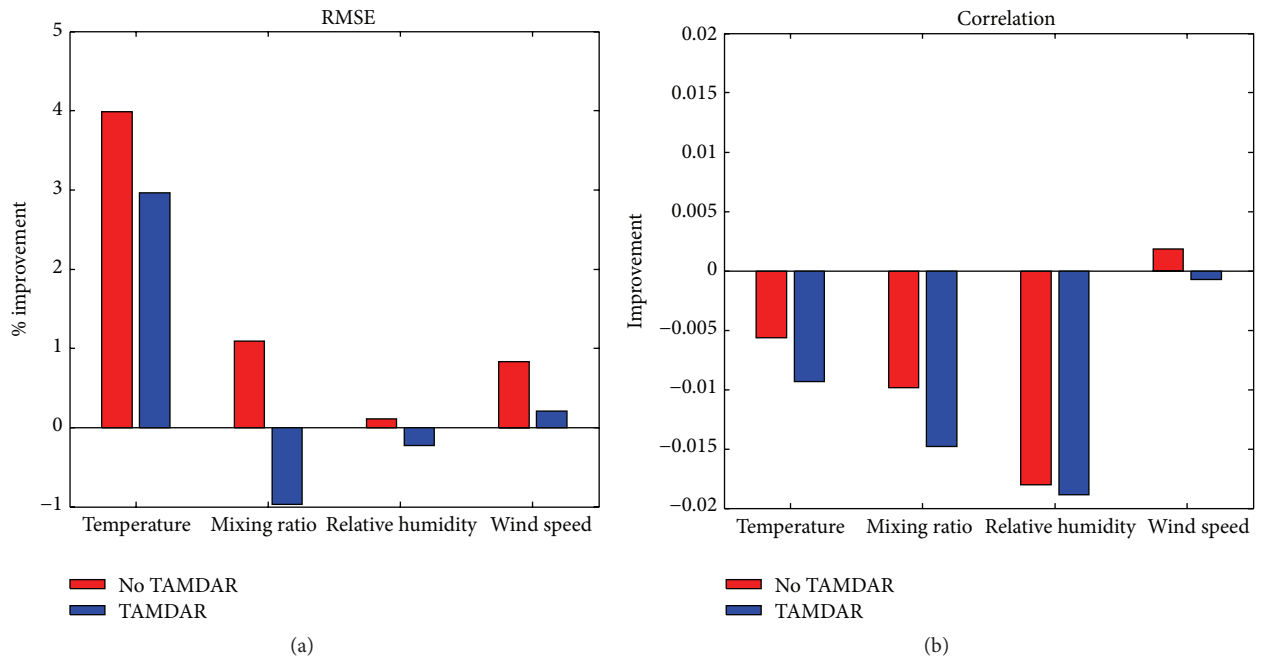

Figure 4: (a) Percentage improvements for root mean squared error (RMSE) and (b) correlation improvement for temperature, mixing ratio, relative humidity, and wind speed due to the resolution increase (without TAMDAR data: red bars; with TAMDAR data: blue bars). The abscissa represents the variables while the ordinate represents the improvement. The statistics are averaged over all sounding locations, vertical levels, and the 6-day (August 1 through August 6) simulation period.

are noted for wind speed (Figures 3(a) and 3(b)). It is unclear why the assimilation of the TAMDAR data results in positive impacts for wind speed in Domain 1 but not in Domain 2 within the 400–600 hPa layer. One possible explanation may be related to the much richer structure and larger gradients of convection simulated by the 4 km domain with the explicit cloud microphysics than the 12 km domain where the activated cumulus parameterization tends to smooth out the fine-scale features of the simulated convective systems. It appears that larger penalty happens on the fine-grid (4 km) domain than the coarse-grid (12 km) domain due to the inevitable spatiotemporal phase errors of the simulated convective systems [47, 48].

Compared to the improvement averaged over the 400–600 hPa layer due to the assimilation of the TAMDAR data, the improvement averaged over the entire layer (not shown) exhibits the only differences in that (a) rather small negative impacts on RMSE are noted for temperature for Domain 2 and (b) small positive impacts on RMSE and correlation are noted for wind speed for Domain 2.

Figure 4 shows the percentage improvements for RMSE and correlation for temperature, mixing ratio, relative humidity, and wind speed due to the resolution increase. For temperature, the resolution increase from 12 km to 4 km has significantly large and positive impacts on reducing the RMSE regardless of whether or not the TAMDAR data are assimilated (Figure 4(a)). This is likely due to the fact that, over the CONUS with complex terrain and heterogeneous surface conditions, the mountains and land/water surfaces exert nontrivial effects on temperature distribution and evolution at local scales and higher-resolution runs are able to resolve such effects much better than coarse resolution runs [26]. In terms of correlation (Figure 4(b)), the resolution increase results in small negative impacts on temperature.

For mixing ratio, the resolution increase has relatively small negative (positive) impacts on reducing the RMSE when the TAMDAR (no TAMDAR) data are assimilated (Figure 4(a)). It is not clear why the resolution increase induces a small negative impact on mixing ratio when the TAMDAR data are assimilated. In terms of correlation improvement for mixing ratio (Figure 4(b)), the resolution increase has relatively large negative impacts no matter whether the TAMDAR data are assimilated or not. Relative humidity exhibits very similar patterns to those of mixing ratio (Figures 4(a) and 4(b)), although the magnitude of the former appears to be smaller (larger) for RMSE percentage improvement (correlation improvement) than the latter. For wind speed, the resolution increase slightly reduces the RMSE (Figure 4(a)) and has nearly negligible impacts on the correlation (Figure 4(b)).

The overall reduction of the RMSE and the deterioration of the correlation with increasing the model resolution are consistent with the fact that progressively detailed mesoscale features are resolved by the 4 km domain with explicit cloud physics than by the 12 km domain. Errors in timing and phases of the small-scale features can greatly penalize the correction [49].

It is interesting to notice that assimilating the TAMDAR data appears to neutralize to a slight degree the positive

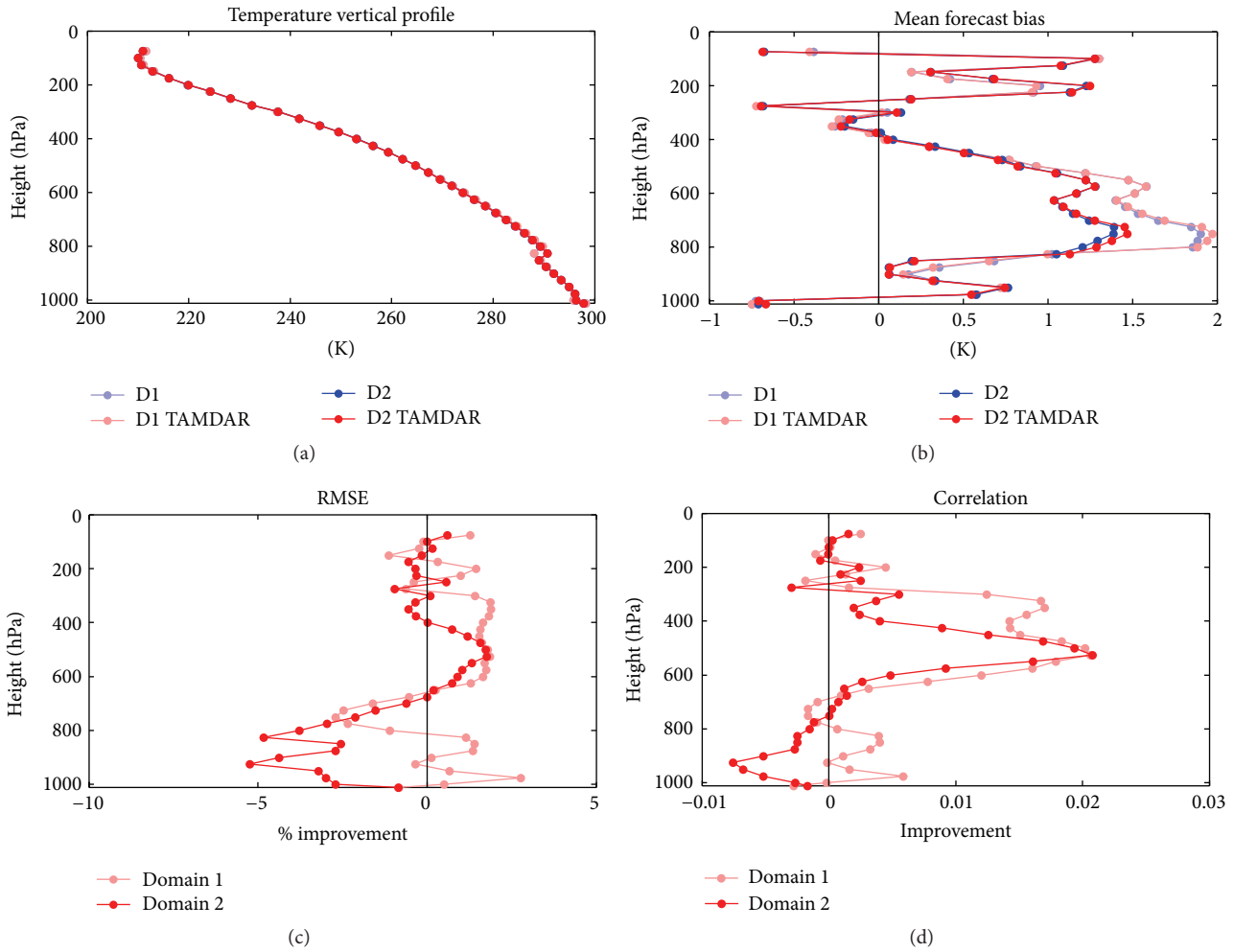

FIGURE 5: Vertical profiles of temperature (a) mean values (K), (b) mean forecast biases (K), (c) percentage improvement for RMSE, and (d) correlation improvement averaged over all locations and simulation period. Red and blue lines in (a) and (b) show model runs without the TAMDAR data and with the TAMDAR data, respectively (Domain 1: light color; Domain 2: dark color). Percentage improvement for RMSE and correlation improvement due to the assimilation of the TAMDAR data for Domain 1 and Domain 2 are represented in (c) and (d) by light and dark red lines, respectively.

impacts from the resolution increase when compared to not assimilating the TAMDAR data (Figure 4). This is also evident in Figure 3 that shows relatively larger positive impacts of assimilating the TAMDAR data for Domain 1 than for Domain 2. All these may suggest that the beneficial effects of the TAMDAR data in high-resolution runs still have not fully emerged and that fine-tuning and optimization according to the model resolution and physical configuration appear to be needed.

4.2. Vertical Distributions. Vertical profiles of mean temperatures, mean forecast biases, percentage improvement for RMSE, and correlation improvement averaged over all sounding locations and over the 6-day simulation period are shown in Figure 5. Here, forecast biases are defined as the mean differences between the simulations and the observations. Temperature mean profiles are identical between Domain 1 and Domain 2 irrespective of whether or not the TAMDAR data are assimilated (Figure 5(a)). Mean forecast biases are also nearly identical between Domain 1 and Domain 2 except for the layer between 500 hPa and 800 hPa where Domain 2 shows smaller positive biases than Domain 1 (Figure 5(b)). It appears that the positive impacts from the resolution increase as seen in Figure 4 have their biggest contributions in the 500 to 800 hPa layer. Noticeable positive improvement for RMSE and correlation due to the assimilation of the TAMDAR data can be seen in the 400 hPa through 600 hPa layer for both domains (Figures 5(c) and 5(d)). For Domain 1, the layer with positive improvement also extends further upward to 300 hPa. Negative improvement for RMSE and correlation can be identified in the layer between the surface and 800 hPa for Domain 2, which could be partly related to the coarse horizontal resolution of the TAMDAR data at low levels (i.e., long distances between airports). Another likely reason is related to the unavoidable errors in timing and phases of the mountain/valley

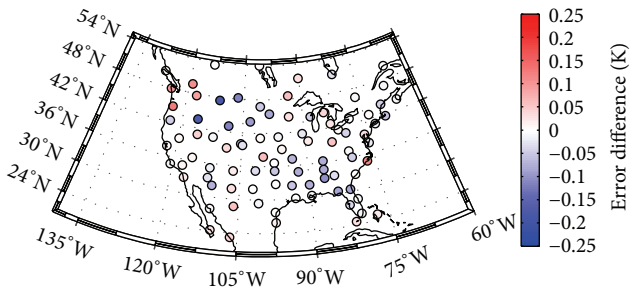

Figure 6: Spatial patterns of the mean absolute error differences in temperature (K) for Domain 1 averaged over the 400 to 600 hPa layer and over the 6-day simulation period. Blue colors indicate improvement of the model biases by assimilating the TAMDAR data while red colors indicate degradation.

and (or) land/sea circulations in the high-resolution runs since a majority of the sounding stations are located over the mountainous western region and along the coasts (see Figure 6).

Averaged over the 400 hPa through 600 hPa levels and over the 6-day simulation period, the spatial pattern of the temperature error differences for Domain 1 (Figure 6) shows positive impacts of assimilating the TAMDAR data on reducing the model biases over a majority of the sounding stations. Here, the error difference is computed for the absolute errors of the two experiments and is defined as follows:

$$\text{Error difference} = \frac{\sum_{i=1}^{n} \left|\text{MOD}^{i}_{\text{TAMDAR}} - \text{OBS}^{i}\right|}{n} - \frac{\sum_{i=1}^{n} \left|\text{MOD}^{i}_{\text{noTAMDAR}} - \text{OBS}^{i}\right|}{n}, \quad (4)$$

where MOD and OBS refer to the model simulations and the observations, respectively, and n represents the number of samples. The spatial pattern of the temperature error differences does not seem to indicate strong area preference regarding positive or negative impacts although the negative impacts tend to show up more along the peripheral areas of the CONUS (Figure 6) where the TAMDAR data also tend to be less. Domain 2 exhibits a similar distribution (not shown) to Domain 1.

For relative humidity, assimilating the TAMDAR data reduces the negative forecast biases for both domains in the middle and lower levers (i.e., 500 hPa to 850 hPa) (Figure 7(b)). This appears to be the direct result of the TAMDAR data adding moisture in those levels (Figure 7(a)). Accordingly, the RMSE and correlation are also improved in the middle and lower levels for both domains (Figures 7(c) and 7(d)). Below 850 hPa, Domain 2 exhibits small biases as well as small impacts but Domain 1 shows large negative impacts around 900 hPa (Figure 7). A rather similar pattern is also found for mixing ratio (not shown). Horizontally, the spatial pattern of the mixing ratio differences for Domain 1 averaged over the 500 to 850 hPa layer and over the 6-day simulation period clearly shows increased moisture over a majority of the sounding stations as a result of assimilating the TAMDAR data (Figure 8).

Vertical profiles of mean wind speeds are very similar between Domain 1 and Domain 2 regardless of whether or not the TAMDAR data are assimilated (Figure 9(a)). Near-surface winds are slightly overestimated by the model for both domains (Figure 9(b)). Above the surface, however, the model underestimates the observed wind speeds with the maximum model biases located around the jet stream layer (~200 hPa). Assimilating the TAMDAR data results in positive improvement for wind speed simulations throughout the model layer for Domain 1 except for the layers near the surface, around 700 hPa and 100 hPa (Figures 9(c) and 9(d)). For Domain 2, positive and negative impacts resulting from assimilating the TAMDAR data on RMSE and correlation of wind speed display a zigzag shape in the vertical, with positive impacts noted primarily for two layers, 200 through 400 hPa and 600 through 800 hPa (Figures 9(c) and 9(d)). These two layers correspond to the layers immediately above and immediately below where the largest positive impacts in temperature are obtained (Figure 5(c)).

To summarize, the above verification results clearly show that within the 400–600 hPa layer assimilating the TAMDAR data consistently results in reduced RMSE and increased correlation for temperature, humidity, and wind speed for both domains with the only exception of wind speed for Domain 2. This once again suggests that the assimilation of the TAMDAR data in high-resolutions RTFDDA system needs to be further optimized.

4.3. Overall Impacts on Surface Variables. Figure 10 shows the percentage improvements for RMSE and correlation improvement for surface pressure, 2 m temperature, 2 m relative humidity, and 10 m wind speed averaged over 500 surface stations and over the 6-day simulation period. The statistics are computed using the hourly observations and the hourly model forecasts. The results suggest that the assimilation of the TAMDAR data does not bring significant impacts on RMSE and correlation at the surface for both domains. One likely reason is that compared to the observations from other sources the TAMDAR data are considerably small in number at and near the surface due to the fact that most TAMDAR data are obtained at very sparsely distributed airports. Another possible reason is that land surface forcing exerts very strong constraints on the surface variables and it needs the combined effect of rather dense observations both at the surface and near the surface to compete with the land surface forcing. In contrast to the negligible impacts on the surface variables related to the assimilation of the TAMDAR data, Figure 10 shows that the resolution increase results in significant improvement for RMSE for all the variables as well as noticeable correlation improvement for temperature and humidity. This is apparently due to the realistic representation of the surface properties and the associated forcing

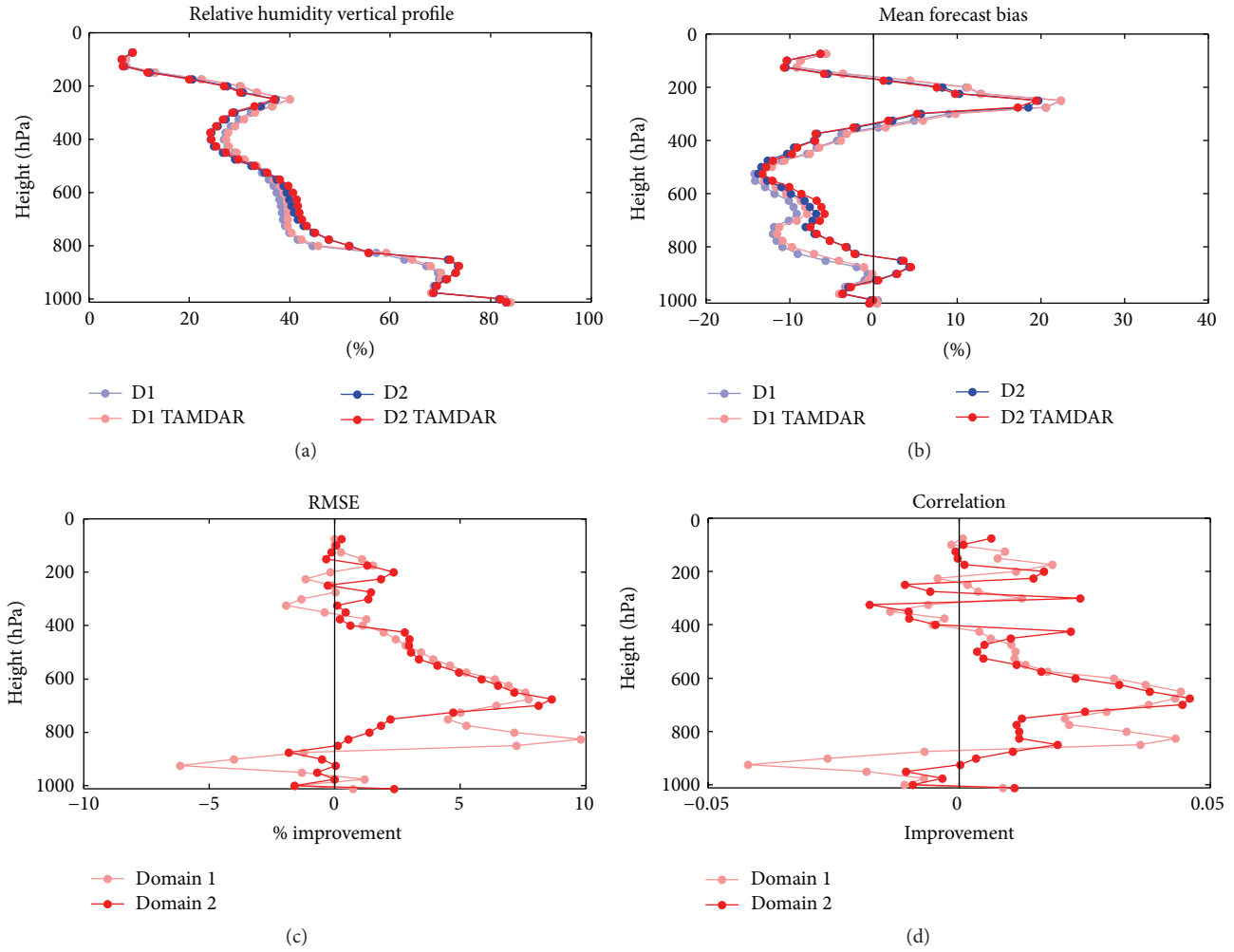

FIGURE 7: The same as Figure 5 except for relative humidity (%).

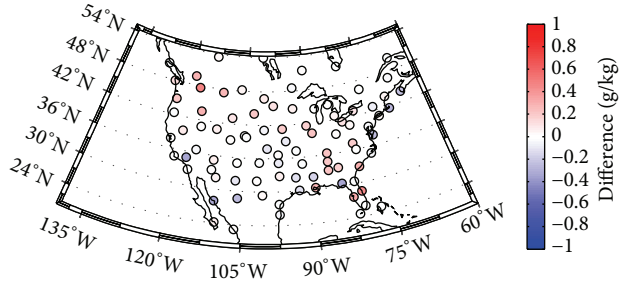

FIGURE 8: Spatial patterns of the mixing ratio differences (g kg^{-1}) for Domain 1 between the runs with and without assimilating the TAMDAR data. The differences are averaged over the 500 to 850 hPa layer and over the 6-day simulation period. Red colors indicate an increase in mixing ratio by assimilating the TAMDAR data while blue colors indicate a decrease.

with a fine-resolution grid. Interestingly, the assimilation of the TAMDAR data results in slight but tangible improvements in surface pressure, temperature, and wind speed on top of the improvements due to the model resolution increase.

5. Conclusions and Discussion

This work examines the impact of assimilating the TAMDAR data as well as the resolution increase on the WRF-based RTFDDA simulations based on 6-day parallel data

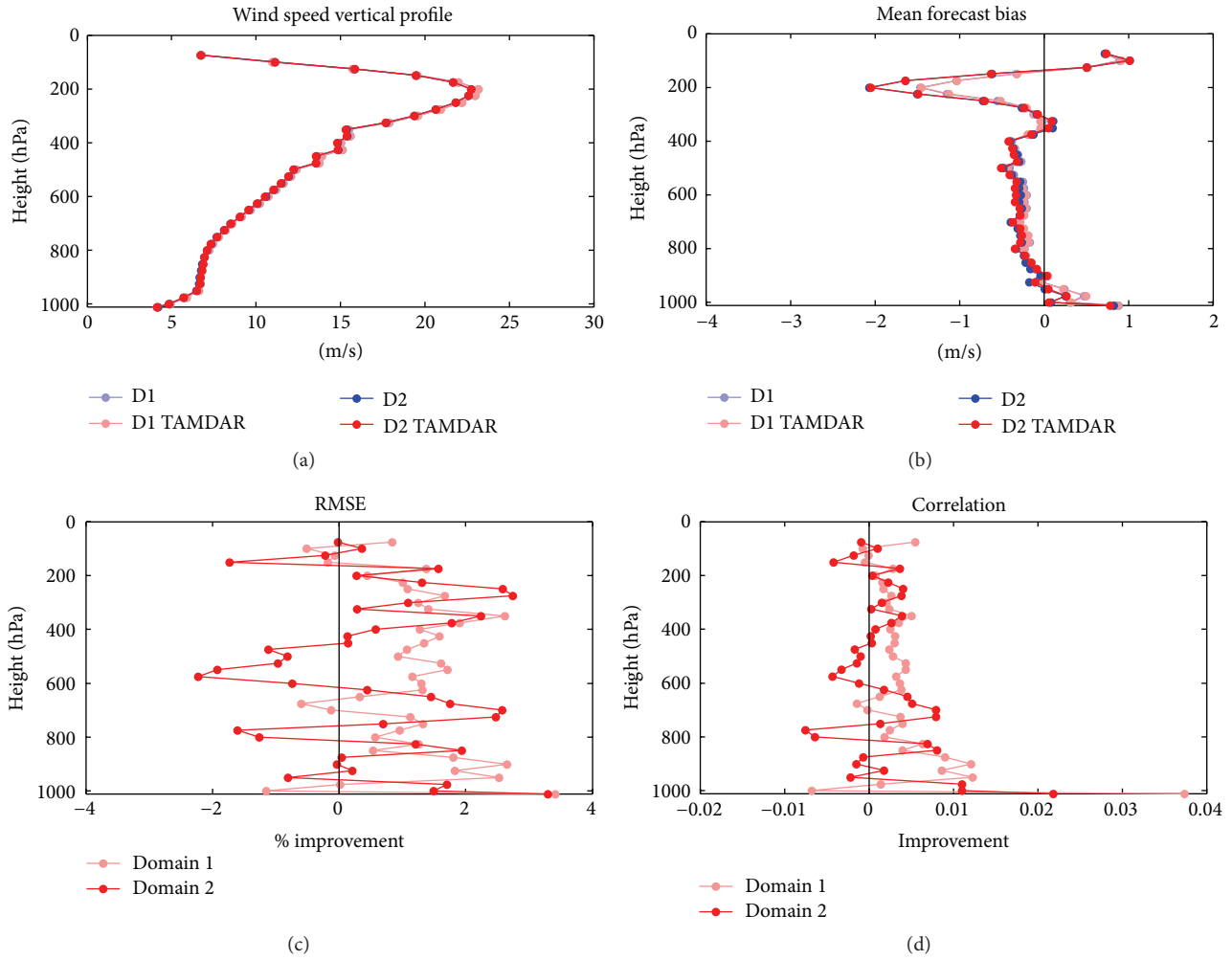

Figure 9: The same as Figure 5 except for wind speed ($m\,s^{-1}$).

assimilation and forecast cycles with the same model configuration as the NCAR-AirDat real-time 12/4 km CONUS operational forecasting system. The verification statistics were computed using all of the 24 h forecasts of the daily cycles during the simulation period and the standard WMO/GTS radiosondes and surface observations.

It is noted that assimilating the TAMDAR data improves the model moisture fields (i.e., relative humidity and mixing ratio) in terms of RMSE and correlation for both the 12 km and 4 km model domains. The TAMDAR data add moisture in the middle and lower levels (500–850 hPa) and reduce the model dry biases. Assimilating the TAMDAR data also improves the simulated temperature at middle to high levels and the simulated wind speed at all levels especially for the 12 km domain.

Increasing the horizontal resolution from 12 km to 4 km has significantly large impacts on the simulated surface variables. The impact of assimilating the TAMDAR data on the surface variables is rather small for both domains during the study period. It is nevertheless noticed that the assimilation of the TAMDAR data brings in small but tangible extra improvements to surface pressure, temperature, and wind speed when the model resolution is increased. Vertically, the temperature forecasts at all levels exhibit the largest positive impacts from the increased horizontal resolution in comparison with the moisture field and wind speed forecasts.

Compared to the previous papers that study the impacts of the TAMDAR data on the model simulations (e.g., [14, 21, 22]), the findings in this work confirm that within the 400–600 hPa layer assimilating the TAMDAR data consistently improves RMSE and correlation for temperature and humidity for both domains and wind speed for Domain 1. Nevertheless, negative impacts for wind speed are identified for this layer for high-resolution Domain 2 and Domain 1 generally shows relatively larger positive impacts of assimilating the TAMDAR data than Domain 2. It has been suggested in this work that the beneficial effects of the TAMDAR data (and possibly other observations) in high-resolution runs might not have been fully explored and realized as yet. It thus becomes necessary to invest and optimize the data assimilation schemes in fine-scale model

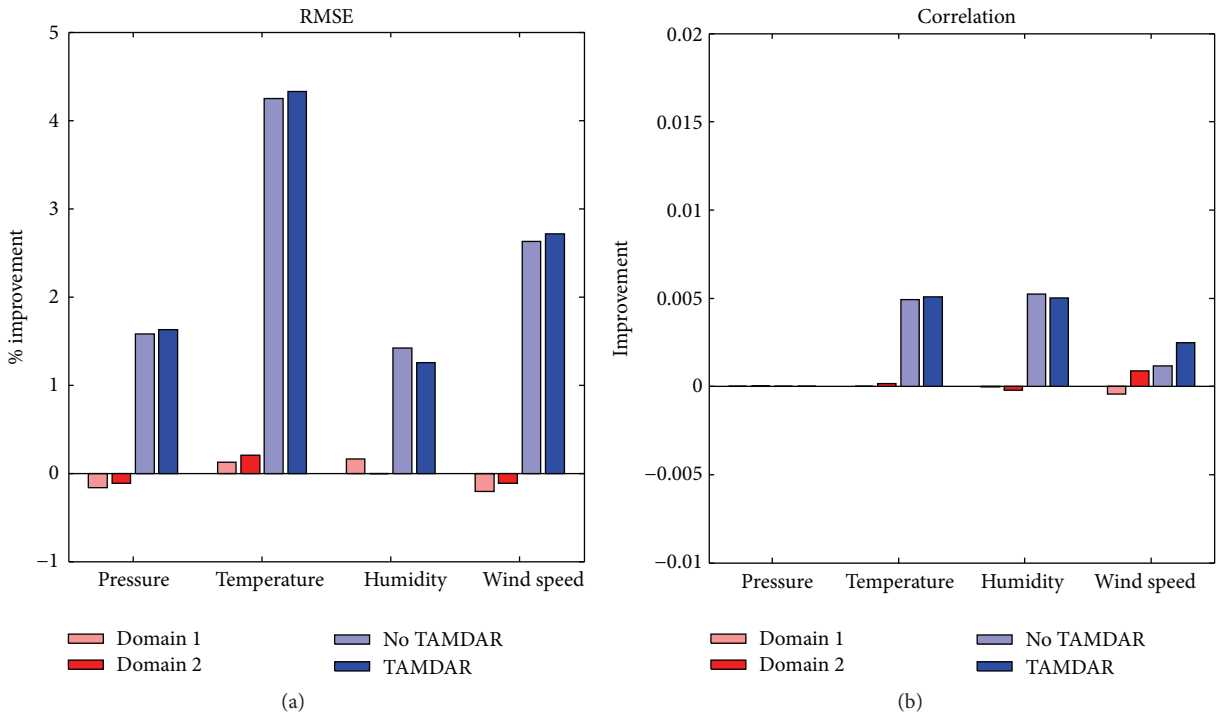

Figure 10: (a) Percentage improvements for root mean squared error (RMSE) and (b) correlation improvement for surface pressure, 2 m temperature, 2 m relative humidity, and 10 m wind speed due to the assimilation of the TAMDAR data and the resolution increase. Red bars indicate improvements due to the TAMDAR data for each domain (Domain 1: light red; Domain 2: dark red) while blue bars indicate improvements due to using higher resolution (without TAMDAR data: light blue; with TAMDAR data: dark blue). The abscissa represents the variables while the ordinate represents the improvement. The statistics are averaged over all surface stations and the 6-day (August 1 through August 6) simulation period.

runs, which is especially true for explicit forecasting of convective systems such as the 4 km RTFDDA model of this study.

Competing Interests

The authors declare that they have no competing interests.

Acknowledgments

This research was funded by the AirDat LLC. The authors thank Allan Huffman, Meredith Croke, Ming Ge, Yuewei Liu, and Francois Vandenberghe for their support and helpful discussions. NCAR is sponsored by the National Science Foundation.

References

[1] R. Daley, *Atmospheric Data Analysis*, Cambridge Atmospheric and Space Science Series, Cambridge University Press, New York, NY, USA, 1991.

[2] E. Kalnay, *Atmospheric Modeling, Data Assimilation and Predictability*, Cambridge University Press, 2003.

[3] S. K. Park and L. Xu, *Data Assimilation for Atmospheric, Oceanic and Hydrologic Applications*, Springer, New York, NY, USA, 2010.

[4] W. R. Moninger, R. D. Mamrosh, and P. M. Pauley, "Automated meteorological reports from commercial aircraft," *Bulletin of the American Meteorological Society*, vol. 84, no. 2, pp. 203–216, 2003.

[5] B. R. Barwell and A. C. Lorenc, "A study of the impact of aircraft wind observations on a large-scale analysis and numerical weather prediction system," *Quarterly Journal of the Royal Meteorological Society*, vol. 111, no. 467, pp. 103–129, 1985.

[6] A. P. M. Baede, P. Kållberg, and S. Uppala, "Impact of aircraft wind data on ECMWF analyses and forecasts during the FGGE period, 8–19 November 1979," *Quarterly Journal of the Royal Meteorological Society*, vol. 113, no. 477, pp. 871–898, 1987.

[7] J. Kruus, "The aircraft to satellite data relay—ASDAR," in *Proceedings of the International Conference on the Results of the Global Weather Experiment*, WMO, WMO Tech. Doc. 107, pp. 145–155, World Meteorological Organization, Geneva, Switzerland, 1986.

[8] S. G. Benjamin, K. A. Brewster, R. Brümmer et al., "An isentropic three-hourly data assimilation system using ACARS aircraft observations," *Monthly Weather Review*, vol. 119, no. 4, pp. 888–906, 1991.

[9] T. L. Smith and S. G. Benjamin, "Relative impact of data sources on a data assimilation system," in *Proceedings of the 10th Conference on Numerical Weather Prediction*, pp. 491–493, American Meteorological Society, Portland, Ore, USA, July 1994.

[10] B. E. Schwartz, S. G. Benjamin, S. M. Green, and M. R. Jardin, "Accuracy of RUC-1 and RUC-2 wind and aircraft trajectory

forecasts by comparison with ACARS observations," *Weather and Forecasting*, vol. 15, no. 3, pp. 313–326, 2000.

[11] T. H. Zapotocny, S. J. Nieman, W. Paul Menzel et al., "A case study of the sensitivity of the Eta data assimilation system," *Weather and Forecasting*, vol. 15, no. 5, pp. 603–621, 2000.

[12] R. J. Graham, S. R. Anderson, and M. J. Bader, "The relative utility of current observation systems to global-scale NWP forecasts," *Quarterly Journal of the Royal Meteorological Society*, vol. 126, no. 568, pp. 2435–2460, 2000.

[13] T. S. Daniels, W. R. Moninger, and R. D. Mamrosh, "Tropospheric Airborne Meteorological Data Reporting (TAMDAR) overview," in *Proceedings of the 10th Conference on Integrated Observing and Assimilation Systems for Atmosphere, Oceans, and Land Surface (IOAS-AOLS '06)*, CD-ROM, P9.1, American Meteorological Society, Atlanta, Ga, USA, January-February 2006.

[14] N. Jacobs, Y. Liu, and C.-M. Druse, "Evaluation of temporal and spatial distribution of TAMDAR data in short-range mesoscale forecasts," in *Proceedings of the 10th Integrated Observing and Assimilation Systems for the Atmosphere, Oceans and Land Surface (IOAS-AOLS '06)*, CD-ROM, P9.11, American Meteorological Society, Atlanta, Ga, USA, February 2006.

[15] W. R. Moninger, T. S. Daniels, and R. D. Mamrosh, "Automatic weather reports from aircraft: TAMDAR and the U.S. AMDAR fleet," in *Proceedings of the 12th Conference on Aviation, Range, and Aerospace*, CD-ROM, P4.2, American Meteorological Society, Atlanta, Ga, USA, January-February 2006.

[16] T. S. Daniels, G. Tsoucalas, M. Anderson, D. Mulally, and W. Moninger, "Tropospheric Airborne Meteorological Data Reporting (TAMDAR) sensor development," in *Proceedings of the 11th Conference on Aviation, Range, and Aerospace*, vol. 7 of *CD-ROM, P7.6*, American Meteorological Society, Hyannis, Mass, USA, October 2002.

[17] Y. Liu, F. Chen, T. Warner, and J. Basara, "Verification of a mesoscale data-assimilation and forecasting system for the Oklahoma City area during the joint urban 2003 field project," *Journal of Applied Meteorology and Climatology*, vol. 45, no. 7, pp. 912–929, 2006.

[18] Y. Liu, W. Yu, F. Vandenberghe, A. Hahmann, T. Warner, and S. Swerdlin, "Assimilation of diverse meteorological datasets with a four-dimensional mesoscale analysis and forecast system," in *Proceedings of the 10th Conference on Integrated Observing and Assimilation Systems for the Atmosphere, Oceans and Land Surface (IOAS-AOLS '06)*, CD-ROM, P2.8, American Meteorological Society, Atlanta, Ga, USA, January-February 2006.

[19] Y. Liu, A. Bourgeois, J. Sun, T. Warner, and S. Swerdlin, "0–12 h forecasts of summer convection using NCAR/RAL obs-nudging based WRF-RTFDDA system," in *Proceedings of the 8th WRF Users Workshop*, Boulder, Colo, USA, June 2007, http://www2.mmm.ucar.edu/wrf/users/workshops/WS2007/presentation/4-7_Liu.pdf.

[20] Y. Liu, N. Jacobs, W. Yu, T. Warner, S. Swerdlin, and M. Anderson, "An OSSE study of TAMDAR data impact on mesoscale data assimilation and prediction," in *Proceedings of the 11th Symposium on Integrated Observing and Assimilation Systems for the Atmosphere, Oceans, and Land Surface (IOAS-AOLS '07)*, J5.20, American Meteorological Society, San Antonio, Tex, USA, January 2007.

[21] W. R. Moninger, S. G. Benjamin, B. D. Jamison, T. W. Schlatter, T. L. Smith, and E. J. Szoke, "Evaluation of regional aircraft observations using TAMDAR," *Weather and Forecasting*, vol. 25, no. 2, pp. 627–645, 2010.

[22] F. Gao, X. Zhang, N. A. Jacobs, X.-Y. Huang, X. Zhang, and P. P. Childs, "Estimation of TAMDAR observational error and assimilation experiments," *Weather and Forecasting*, vol. 27, no. 4, pp. 856–877, 2012.

[23] H. L. Wang and X.-Y. Huang, "TAMDAR observation assimilation in WRF 3D-Var and its impact on hurricane Ike (2008) forecast," *Atmospheric and Oceanic Science Letters*, vol. 5, no. 3, pp. 206–211, 2015.

[24] M. Croke, N. Jacobs, P. Childs et al., "Preliminary verification of the NCAR-AirDat operational RTFDDA-WRF system," in *Proceedings of the 14th Integrated Observing and Assimilation Systems for the Atmosphere, Oceans and Land Surface (IOAS-AOLS '10)*, 8.5, American Meteorological Society, Atlanta, Ga, USA, January 2010.

[25] Y. Liu, Y. Zhang, W. Wu et al., "Evaluation of TAMDAR data impact on predicting warm-season convection using the NCAR-AirDat WRF-based RTFDDA system," in *Proceedings of the 14th Conference on Integrated Observing and Assimilation Systems for the Atmosphere, Oceans and Land Surface (IOAS-AOLS '10)*, American Meteorological Society, Atlanta, Ga, USA, January 2010.

[26] M. L. Weisman, W. C. Skamarock, and J. B. Klemp, "The resolution dependence of explicitly modeled convective systems," *Monthly Weather Review*, vol. 125, no. 4, pp. 527–548, 1997.

[27] J. S. Kain, "The Kain-Fritsch convective parameterization: an update," *Journal of Applied Meteorology*, vol. 43, no. 1, pp. 170–181, 2004.

[28] J. S. Kain and J. M. Fritsch, "A one-dimensional entraining/detraining plume model and its application in convective parameterization," *Journal of the Atmospheric Sciences*, vol. 47, no. 23, pp. 2784–2802, 1990.

[29] J. S. Kain and J. M. Fritsch, "Convective parameterization for mesoscale models: the Kain-Fritsch scheme," in *The Representation of Cumulus Convection in Numerical Models*, K. A. Emanuel and D. J. Raymond, Eds., p. 246, American Meteorological Society, Boston, Mass, USA, 1993.

[30] Y.-L. Lin, R. D. Farley, and H. D. Orville, "Bulk parameterization of the snow field in a cloud model," *Journal of Climate and Applied Meteorology*, vol. 22, no. 6, pp. 1065–1092, 1983.

[31] S. A. Rutledge and P. V. Hobbs, "The mesoscale and microscale structure and organization of clouds and precipitation in midlatitude cyclones. XII: a diagnostic modeling study of precipitation development in narrow cloud-frontal rainbands," *Journal of the Atmospheric Sciences*, vol. 20, pp. 2949–2972, 1984.

[32] W.-K. Tao, J. Simpson, and M. McCumber, "An ice-water saturation adjustment," *Monthly Weather Review*, vol. 117, no. 1, pp. 231–235, 1989.

[33] S.-Y. Hong and H.-L. Pan, "Convective trigger function for a mass-flux cumulus parameterization scheme," *Monthly Weather Review*, vol. 126, no. 10, pp. 2599–2620, 1998.

[34] G. Grell, J. Dudhia, and D. R. Stauffer, "A description of the fifth-generation Penn State/NCAR mesoscale model (MM5)," NCAR Tech. Note NCAR/TN-398+IA, National Center for Atmospheric Research, 1995.

[35] J. M. Cram, Y. Liu, S. Low-Nam et al., "An operational mesoscale RTFDDA analysis and forecasting system," in *Proceedings of the 18th Conference on Weather Analysis and Forecasting and 14th Conference on Numerical Weather Prediction*, CD-ROM, J2.11, American Meteorological Society, Fort Lauderdale, Fla, USA, 2001.

[36] Y. Liu, T. T. Warner, J. F. Bowers et al., "The operational mesogamma-scale analysis and forecast system of the U.S. army

test and evaluation command. Part I: overview of the modeling system, the forecast products, and how the products are used," *Journal of Applied Meteorology and Climatology*, vol. 47, no. 4, pp. 1077–1092, 2008.

[37] D. R. Stauffer and N. L. Seaman, "Multiscale four-dimensional data assimilation," *Journal of Applied Meteorology*, vol. 33, no. 3, pp. 416–434, 1994.

[38] C. Davis, T. Warner, E. Astling, and J. Bowers, "Development and application of an operational, relocatable, mesogamma-scale weather analysis and forecasting system," *Tellus A*, vol. 51, no. 5, pp. 710–727, 1999.

[39] T. T. Warner and H.-M. Hsu, "Nested-model simulation of moist convection: the impact of coarse-grid parameterized convection on fine-grid resolved convection," *Monthly Weather Review*, vol. 128, no. 7 I, pp. 2211–2231, 2000.

[40] D. L. Rife, T. T. Warner, F. Chen, and E. G. Astling, "Mechanisms for diurnal boundary layer circulations in the Great Basin Desert," *Monthly Weather Review*, vol. 130, no. 4, pp. 921–938, 2002.

[41] D. L. Rife, C. A. Davis, Y. Liu, and T. T. Warner, "Predictability of low-level winds by mesoscale meteorological models," *Monthly Weather Review*, vol. 132, no. 11, pp. 2553–2569, 2004.

[42] T. T. Warner, J. F. Bowers, S. P. Swerdlin, and B. A. Beitler, "A rapidly deployable operational mesoscale modeling system for emergency-response applications," *Bulletin of the American Meteorological Society*, vol. 85, no. 5, pp. 709–716, 2004.

[43] Y. Liu, T. T. Warner, E. G. Astling et al., "The operational mesogamma-scale analysis and forecast system of the U.S. Army Test and Evaluation Command. Part II: interrange comparison of the accuracy of model analyses and forecasts," *Journal of Applied Meteorology and Climatology*, vol. 47, no. 4, pp. 1093–1104, 2008.

[44] R. D. Sharman, Y. Liu, R.-S. Sheu et al., "The operational mesogamma-scale analysis and forecast system of the U.S. Army Test and Evaluation Command. Part III: forecasting with secondary-applications models," *Journal of Applied Meteorology and Climatology*, vol. 47, no. 4, pp. 1105–1122, 2008.

[45] Y. Liu, J. Hacker, G. Roux et al., "WRF 'obs-nudging' updates, verification and plans for the future developments," in *Proceedings of the 9th WRF User Workshop*, P1.7, Boulder, Colo, USA, June 2008, http://www2.mmm.ucar.edu/wrf/users/workshops/WS2008/presentations/1-7.pdf.

[46] W. C. Skamarock, J. B. Klemp, J. Dudhia et al., "A description of the advanced research WRF version 2," NCAR Technical Note NCAR/TN-468+STR, 2006.

[47] C. A. Davis, B. Brown, and R. Bullock, "Object-based verification of precipitation forecasts. Part I: methodology and application to mesoscale rain areas," *Monthly Weather Review*, vol. 134, no. 7, pp. 1772–1784, 2006.

[48] C. Davis, B. Brown, and R. Bullock, "Object-based verification of precipitation forecasts. Part II: application to convective rain systems," *Monthly Weather Review*, vol. 134, pp. 1785–1795, 2006.

[49] C. F. Mass, D. Ovens, K. Westrick, and B. A. Colle, "Does increasing horizontal resolution produce more skillful forecasts?" *Bulletin of the American Meteorological Society*, vol. 83, no. 3, pp. 407–430, 2002.